

# ULTRASONIC CHARACTERIZATION OF STRUCTURAL PROPERTIES OF ORIENTED STRANDBOARD: A COMPARISON OF DIRECT-CONTACT AND NON-CONTACT METHODS<sup>1</sup>

*Ronnie Y. Vun†*

Graduate Research Assistant

*Qinglin Wu†*

Associate Professor

Louisiana Forest Products Laboratory  
School of Renewable Natural Resources  
Louisiana State University Agricultural Center  
Baton Rouge, LA 70803

*Mahesh C. Bhardwaj*

Research and Development Director

and

*Gary Stead*

President

SecondWave Systems Corporation  
1020 East Boal Avenue  
Boalsburg, PA 16827

(Received January 2002)

## ABSTRACT

A through-thickness ultrasonic transmission (UT) in oriented strandboard (OSB) was done to compare the performance of direct-contact (DC) and non-contact (NC) ultrasonic systems. The DC measurements produced a higher velocity than the NC system for a given board type, possibly due to transducer's compression over liquid couplant in the DC method. The UT responses correlated non-linearly to sample density. The responses were not affected by the panel shelling ratio for the three-layer boards. Viable correlations between panel properties and UT parameters were board-specific for either method. Attenuation and root means square voltage (RMS) parameters were suitably used as density predictors if the flake alignment level is known; otherwise, velocity parameter could be used. In the single-layer boards, internal bond strength, bending stiffness, and breaking resistance were highly correlated to attenuation and RMS, a calibration importance. A density of 900 kg/m<sup>3</sup> marked the transition point for the UT responses. The point showed the transition between the diminishing physical effects of the interspatial voids in the lower density half and the increasing plastic-strain hardening modifications in the higher density half. The high correlations of DC-Velocity and NC-Attenuation to density and strength properties attest a feasible application of both methods in wood composite research and in a real-time quality control system for fiber-based facilities.

**Keywords:** Densification, direct-contact, non-contact ultrasound, quality control, OSB, velocity, attenuation.

## INTRODUCTION

Oriented strandboard (OSB) is one of the modern structural wood composites widely

used as sheathing, flooring, and I-joist materials in house construction. OSB consists of wood strands or flakes glued with an exterior-type, waterproof resin. Mat layering and alignment of wood flakes are used to improve mechanical properties of the board. The mat formation by depositing resin-coated flakes re-

---

<sup>1</sup> This paper (NO: 02-40-0457) is published with the approval of the Director of the Louisiana Agricultural Experiment Station.

† Member of SWST.

sults in relatively loosely packed mats. Although mat density increases during hot pressing, the final product still contains a substantial volume of voids (Furuno et al. 1983). Understanding the void structure created by the interactions of raw material and mat formation parameters has many important implications for evolution of the optimal properties into a quality product. In particular, the presence of voids in OSB reduces its elastic moduli and affects its dimensional stability (Lenth and Kamke 1996; Wu 1999). Therefore, attention must be given to the void distribution and its effects on product performance.

Voids are strong scatters of elastic waves. Various nondestructive techniques have been used to quantify voids and their effects on panel properties in polymer composites (Judd and Wright 1978). Among these methods, ultrasonic transmission (UT) is the most generally useful technique at present (Chen and Beall 2000; Vun et al. 2000; Jeong 1997; Jeong and Hsu 1995). The method involves transmitting a short pulse of ultrasonic energy through the specimen, measuring the attenuation caused by passage through the material, and defining the maximum acceptable void content in terms of ultrasonic attenuation (Judd and Wright 1978). This method has an advantage over conventional approaches in that it can be used to assess the whole panel rather than only a small portion.

The need for application of nondestructive evaluation (NDE) technologies to improve the understanding of material characteristics (i.e., defects, basic properties, geometry, bonding quality, etc.) for wood composites has been overwhelmingly driven from technology push to market pull (Beall 1996a). However, effective applications of the technologies in the necessary operating conditions with reasonable accuracy should be supported with knowledge of material responses obtained from system calibration. In studying wood composites, the NDE is beset with intrinsic material problems such as high attenuation and dispersion, anisotropy, growth properties, and heterogeneity of boundaries (Beall

1996b). In addition, coupling of transducers to wood-based materials as used in the direct-contact (DC) system presents the greatest source of variability and the major impediment to on-line implementation of NDE in processing wood-based materials (Ermolov 1998). The factors that affect coupling efficiency include acoustic impedance match of the transducers to the substrate, type of couplants between the transducer and the substrate, and characteristic of the substrate. Thus, the success of UT techniques depends largely on the couplants, including grease/gel couplants, adhesives, elastomerics, and air, and the coupling process.

With the advent of high transduction transducers used in non-contact (NC) ultrasonics, the exorbitant acoustic impedance barriers between air and most materials can be resolved (Bhardwaj 1997). This has resulted in a more sensitive NC air-coupling than the gel-coupling technique. Ultrasound technologies have been widely used today as compared to X-ray and  $\gamma$ -ray methods because of their cost-effectiveness, portability, non-hazardousness, and applicability to all states except plasma and vacuum of matters (Bhardwaj et al. 2000).

For a proper application of the UT techniques in a complex wood composite such as OSB, the effect of void content as influenced by board density on ultrasonic responses and panel properties needs to be investigated. The objectives of this work were (1) to investigate the feasibility of using DC and NC ultrasonic systems for measuring OSB properties as influenced by panel density, flake alignment level, and layering structures; and (2) to establish relationships among the processing variables that determine the material behavior of the boards and UT parameters such that calibration models can be developed for both ultrasonic systems.

## EXPERIMENTAL PROCEDURES

### *Specimen preparation*

Using aspen flakes and liquid phenol-formaldehyde resin, single- and three-layer OSB

panels were fabricated for the study (Wu 1999; Lee and Wu 2002). Panels in each type were made with 0.5% wax at the 4% RC level (based on oven-dry weight of the wood flakes) in two replicates. The single-layer boards had four nominal densities (450, 650, 850, and 1150 kg/m<sup>3</sup>), and three alignment levels. The three-layer boards had four shelling ratios (represented by flake weight ratio, FWR, between the face layers and the entire panel), and two alignment levels. The single-layer panels (610 × 610 × 13 mm) were prepressed to thickness prior to heating of the mats for resin curing at 190°C for 6 min. The three-layer panels (610 × 610 × 13 mm) were made with a conventional pressing procedure (one-min closing and 6-min pressing time at 190°C). After hot pressing, the panels were conditioned and edge-trimmed. Based on the measured flake angles from panel surface, flake alignment levels were quantified using percent of alignment (Geimer 1979). The flake alignment level was classified into three categories: (1) high alignment level (HAL), which ranged from 76 to 85%, (2) low alignment level (LAL), from 56 to 59%, and (3) random alignment level (RAL), from 22 to 29%. Ten base specimens (51 × 51 × 13 mm) were randomly selected and cut from each panel replicate, giving a total of twenty samples at each condition. The major flake alignment direction of the panel was marked on the top surface of each sample. The specimens were conditioned at 24°C and 60% relative humidity prior to the UT testing to reach an average equilibrium moisture content of 7.2% for all panels. Thereafter, the specimens were destructively evaluated for the mechanical properties.

#### *Direct-contact transmission*

Direct-contact UT measurements were taken in a through-transmission mode with two Panametrics 100-kHz transducers—coupled on each opposite surface of the specimen using silicon gel (Fig. 1a) and a constant pressure under 3-kg weight. A Panametrics 5058 Pulser/Receiver was used to generate a 400-volt impulse that excites one transmitting

transducer, and the other transducer captures the transmitted signal. Equipment calibration settings, including gain, damping, pulse height, pulser gain, and attenuator, were selected to cover the whole density range of the specimens tested. With a consistent setting of 40–60 dB gain or 0–80 dB attenuator, 30-dB preamplified signals were sampled at a rate of 5 MHz, and the signals were digitized by a GageScope 8-bit CS225 card and processed by a signal processing software.

Velocity, impedance, attenuation, and root mean square (RMS) voltage of the DC ultrasound parameters were used to characterize the properties of the OSB (Vun 1998). The through-thickness velocity,  $V$ (m/s), is the ratio between sample thickness and signal transit time:

$$V = d/t \quad (1)$$

where  $d$  is the sample thickness (mm) and  $t$  is the signal transit time ( $\mu$ s) across the thickness. The impedance of the material determines the alternating current of stress waves that flows through the material. As an analog to a given alternating current potential difference, the impedance of the ultrasonic current is affected by difference in sample density (Benson 1991). The material impedance,  $Z$  (Gg/s.m<sup>2</sup>), is then calculated by

$$Z = V \cdot \rho \quad (2)$$

where  $\rho$  is the sample density (10<sup>-3</sup> kg/m<sup>3</sup>). Attenuation is the energy loss associated with a decrease in the wave amplitude scattered by discontinuity and absorption among the different densities. Attenuation,  $\alpha$ (dB), is given by

$$\alpha = 20 \text{ Log}(A/A_{ref}) \quad (3)$$

where  $A$  is the peak amplitude (v), and  $A_{ref}$  is the maximum amplitude allowable by the system (i.e., 5.2 volts). The RMS voltage represents the signal intensity of the acquired signal (Beauchamp and Yuen 1979), which is measured on a linear scale in voltage and computed by time-averaging rectification as

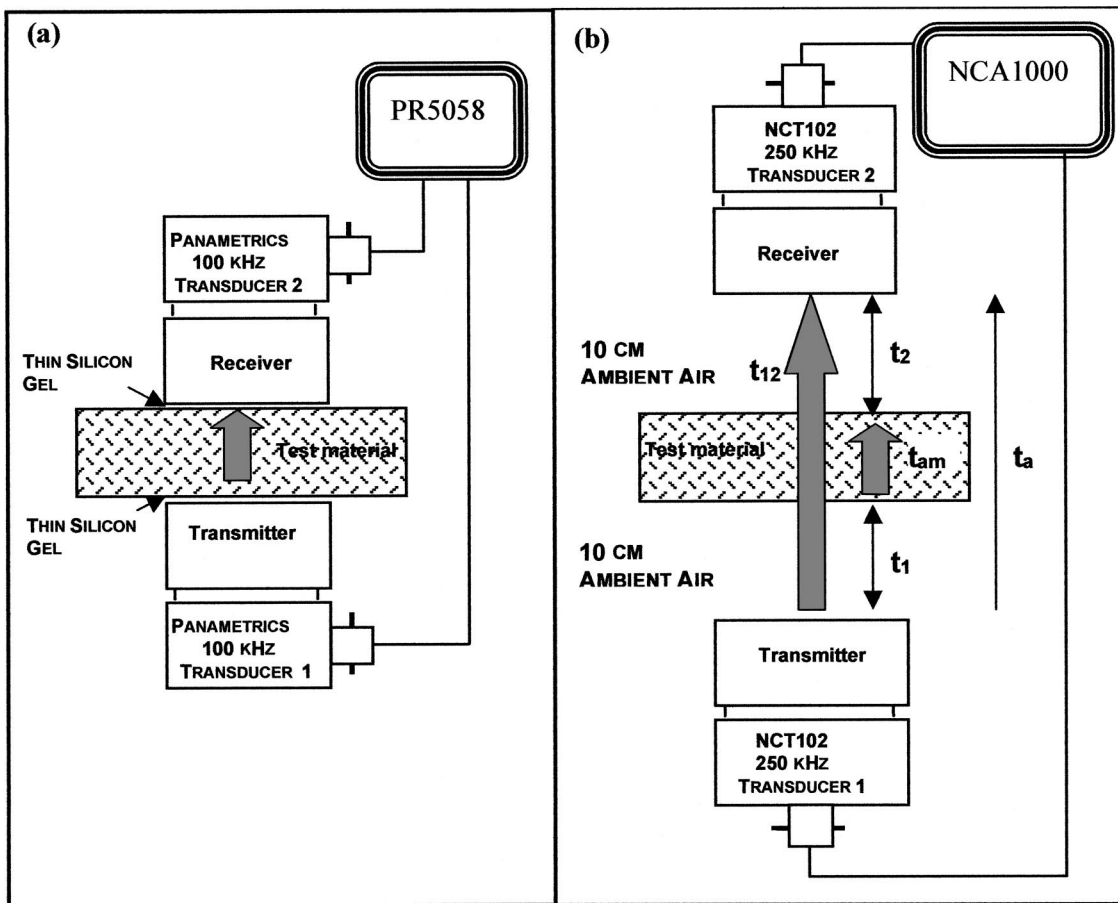


Fig. 1. Experimental setup for direct-contact (a) and non-contact (b) ultrasonic systems.

$$\text{RMS} = \left( \frac{1}{\Delta t} \int v^2(t) dt \right)^{1/2} \quad (4)$$

where  $\Delta t$  is the time interval ( $\mu\text{s}$ ) and  $v$  is the voltage.

#### Non-contact transmission

A SecondWave NCA1000-2E, non-contact ultrasonic system equipped with two 250-kHz, 25-mm NCT102 transducers was used for the NC through-thickness measurements (Fig. 1b). The system uses a deconvolved-chirp specially synthesized to characterize the acoustic impedance of the piezoelectric matching layer, which generates a high air-transduction necessary for NC ultrasound propagation in test materials (Bhardwaj et al. 2000).

The system computes sample thickness and ultrasound velocity according to:

$$d_m = V_a \cdot t_{am} = V_a \cdot [t_a - (t_1 + t_2)/2] \quad (5)$$

$$V_m = \frac{d_m}{[t_{am} - (t_a - t_{12})]} \quad (6)$$

where  $V_m$  is the ultrasound velocity through the test material (m/s),  $V_a$  is the reference ultrasound velocity in air (m/s),  $d_m$  is the material thickness (m),  $t_{am}$  is the time of flight (ToF) in air relative to material thickness (s),  $t_a$  is the ToF of direct transmission in the air column (s),  $t_1$  is the reflected round trip ToF from transducer 1 to the bottom surface of the material (s),  $t_2$  is the reflected round trip ToF from transducer 2 to the top surface of the

material (s), and  $t_{12}$  is the ToF through air column when material is in between transducer 1 and transducer 2 (Fig. 1b).

The attenuation energy is determined by the integrated response (IR). IR (dB) is the net power of the actual ultrasound energy transmitted through the material as evaluated by:

$$IR_m = IR_a - IR_{12} \quad (7)$$

where  $IR_m$  is the integrated response of the peak energy transmitted in the material,  $IR_a$  is the IR in air, and  $IR_{12}$  is the IR in air when the material is in between the transducers. Being frequency independent, IR is related to the transmission coefficient ( $T$ ) that measures how ultrasound is transmitted from one medium to another, given by:

$$T = \frac{Z_1 Z_2}{(Z_1 + Z_2)^2} \quad (8)$$

where  $Z_1$  and  $Z_2$  are the acoustic impedance of ultrasonic propagation in medium 1 and medium 2, respectively.  $IR_m$  is related to  $T$  as

$$IR_m = 20 \text{ Log}(T) \quad (9)$$

The variable  $IR_m$  provides information on internal material quality such as degree of bonding, nature of the microstructure and texture, absence or presence of phases, and type of inclusions in the material (Bhardwaj 1997; Bhardwaj et al. 2000).

The UT measurement with the NCA1000 analyzer was done as follows. After the transducers were aligned, the equipment was calibrated to a known air ultrasound velocity of 344–346 m/s and a reference specimen, a 25.4-mm transparent polystyrene having 21.75  $\mu$ s round trip ToF and 2320 m/s material velocity under ambient conditions. From the first peak analysis, gates were created forming four ultrasonic paths of propagation. These paths were P1: transducer 1 to transducer 2, P2: transducer 1 to material bottom surface reflection, P3: transducer 2 to material top surface reflection, and P4: transducer 2 to transducer 1. Then, based on the reference velocity and thickness, the velocity, thickness, and ToF of

the test materials were computed and displayed.

### Panel density and density profile

Vertical (thickness) and horizontal (length or width) density profiles of each specimen were mapped using a Quintek Density Profiler (QDP-01X) after UT measurements. The maximum, average, and minimum densities along each direction were evaluated from the measured profiles for each sample.

### Mechanical properties

After UT and density measurements, each base specimen was ripped to obtain two *in-situ* 51  $\times$  13  $\times$  13-mm bending samples with the largest dimension of each sample parallel to the major flake alignment direction, and a 51  $\times$  25  $\times$  13-mm sample for testing internal bond (IB) strength. All tests were conducted with a 4260 Instron machine according to the ASTM-D1037. The IB tests were done at a strain rate of 1 mm/min; whereas the modulus of elasticity (MOE) and modulus of rupture (MOR) of each sample were measured with a 6 mm/min loading rate. Each failed specimen was oven-dried to determine its moisture content at the testing time. IB (MPa), bending stiffness (E·I, MPa.cm<sup>4</sup>), and breaking resistance (R·S, MPa.cm<sup>3</sup>) were computed as:

$$IB = \frac{P}{bL} \quad (10)$$

$$E \cdot I = MOE \frac{bh^3}{12} \quad (11)$$

$$R \cdot S = MOR \frac{bh^2}{6} \quad (12)$$

where P is the peak load from the IB test (N), E is the MOE (MPa), I is the moment of inertia given by  $I = bh^3/12$  (cm<sup>4</sup>), R is the MOR (MPa), S is the section modulus given by  $S = bh^2/6$  (cm<sup>3</sup>), and b, h, and L are the width, height, and length (cm) of the specimen, respectively.



### Statistical analysis

SAS (2000) software was used to perform analysis of variance (ANOVA) with the Bonferroni adjustment for multiple comparisons of the class groups. The measured ultrasonic parameters, density, and strength are segregated by resin content, flake alignment, board type (i.e., single layer versus three layers), and UT methods. A backward elimination option was used in the model selection procedure to evaluate the sensitivity of the variables to the high and low densities in the vertical and horizontal directions. Scatter plots with the appropriate regressions (polynomial or power) were used to establish the correlations among density, strength properties, acoustic velocity, attenuation, and RMS.

## RESULTS AND DISCUSSIONS

### Density profile and basic properties

Typical density profiles for the single- and three-layer boards are shown in Fig. 2. As expected, the single-layer boards had relatively uniform vertical density profiles with an overall density variation of  $\pm 75 \text{ kg/m}^3$  about the mean. The uniform profile was attributed to the prepressing prior to mat heating during hot pressing (Wu 1999). For the single-layer panels (Table 1), the general trend of the mechanical properties is an increase with density at all flake alignment levels. MOE, MOR, and IB strength increased as the flake alignment level increased from low to high. The same trends were also observed with the DC velocity. For both methods, the UT velocity increased and UT attenuation decreased as the sample density increased.

In the three-layer boards, the M-shape density profiles (Fig. 2b) showed a high surface density and a low core density that led to an overall density variation of  $\pm 144 \text{ kg/m}^3$  about the mean. The average MOR (29.4 MPa) of the three-layer panels was significantly lower than that of the single-layer panels (44.5 MPa, excluding the random panels). This was caused by the low-density core layer in the three-layer panels. The panel shelling ratio had

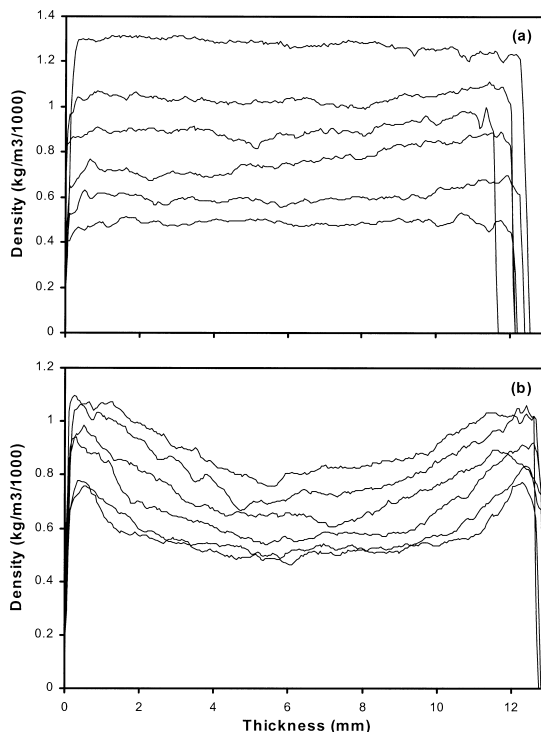


Fig. 2. Typical density profiles of single- (a) and three-layer (b) OSB used in the study.

significant effects on MOR and MOE panels (Table 2). However, its effect on all ultrasonic variables was insignificant. Also, the ultrasonic variables were not affected by differences in flake alignment levels for the boards.

### Velocity-density correlation

The UT velocity in the single-layer boards (Table 1) was generally higher than that of the three-layer boards (Table 2) at a similar density. This was due to difference in the density profile and layering structure between the board types. With a wider density range (465–1400  $\text{kg/m}^3$ ), the single-layer panels had a higher correlation between the UT velocity and density than the three-layer panels (Table 3). The velocity from both methods responded poorly in the three-layer panels with a narrow density range (600–825  $\text{kg/m}^3$ ) among the boards.

The DC method produced a consistently

TABLE 1. Mechanical and ultrasonic properties for the single-layer boards at the 4% RC level.

Board <sup>c</sup> type	Density (kg/m <sup>3</sup> )	Mechanical properties <sup>b</sup>				Ultrasonic properties <sup>d</sup>						
		MOR (MPa)	MOE (MPa)	RS (MPa-cm <sup>3</sup> )	EI (MPa-cm <sup>4</sup> )	IB (MPa)	DCV (m/s)	DCA (-dB)	DCR (v)	DCZ (Mg/s-m <sup>2</sup> )	NCV (m/s)	NCA (-dB)
HAL	594	30.4	243	9.9	51	0.64	810	28.25	0.31	481	610	83.0
	(5) <sup>a</sup>	(2.1)	(20)	(0.6)	(5)	(0.18)	(112)	(5.5)	(0.06)	(67)	(7)	(6.1)
	783	46.0	485	14.2	94	1.12	920	7.11	0.88	709	770	66.7
	(79)	(6.3)	(133)	(2.0)	(26)	(0.18)	(61)	(6.0)	(0.28)	(127)	(66)	(2.2)
	1043	65.1	1056	21.2	213	1.43	1326	1.23	1.11	1222	905	71.3
	(41)	(5.6)	(214)	(2.2)	(46)	(0.05)	(160)	(0.4)	(0.07)	(375)	(83)	(4.1)
LAL	1207	68.4	1296	23.0	275	1.47	1257	0.75	1.23	1426	1075	84.0
	(42)	(1.6)	(160)	(0.5)	(28)	(0.25)	(126)	(0.5)	(0.10)	(228)	(207)	(6.0)
	562	21.0	185	7.0	40	0.57	748	32.13	0.24	421	1046	87.8
	(22)	(1.5)	(12)	(0.7)	(3)	(0.12)	(32)	(7.5)	(0.11)	(22)	(364)	(5.0)
	808	41.4	447	12.9	87	0.85	847	2.30	1.00	684	693	68.7
	(50)	(3.1)	(67)	(0.9)	(13)	(0.14)	(18)	(1.2)	(0.11)	(45)	(39)	(3.6)
RAL	1013	56.7	961	18.1	190	1.16	1270	1.56	1.07	1288	853	79.3
	(55)	(8.0)	(196)	(3.0)	(43)	(0.12)	(47)	(1.7)	(0.17)	(113)	(77)	(2.6)
	1251	64.9	1213	20.3	237	1.28	1308	1.35	1.13	1636	1103	86.7
	(6)	(15)	(406)	(4.5)	(78)	(0.07)	(171)	(0.8)	(0.14)	(210)	(274)	(8.1)
	570	9.9	122	3.2	25	0.48	707	29.03	0.30	407	638	83.0
	(46)	(2.9)	(31)	(1.1)	(8)	(0.04)	(99)	(7.0)	(0.10)	(87)	(56)	(6.0)
RAL	817	30.1	376	9.1	71	1.13	919	3.74	1.01	752	724	72.5
	(57)	(5.7)	(77)	(1.7)	(14)	(0.08)	(108)	(3.5)	(0.17)	(123)	(75)	(3.1)
	925	36.0	509	12.0	106	1.02	950	3.75	0.92	882	721	73.3
	(84)	(8.8)	(264)	(2.6)	(49)	(0.24)	(54)	(2.5)	(0.14)	(125)	(51)	(3.1)

<sup>a</sup> Values in parenthesis are the Standard Deviation.

<sup>b</sup> MOR = Modulus of rupture (MPa), MOE = Modulus of elasticity (MPa), RS = Breaking resistance (MPa-cm<sup>3</sup>), EI = Bending stiffness (MPa-cm<sup>4</sup>), IB = Internal bonding strength (MPa).

<sup>c</sup> HAL = High alignment level ~80%, LAL = Low alignment level ~58%, RAL = Random alignment level ~26%.

<sup>d</sup> DC = Direct-Contact Method, NC = Non-Contact Method, -V = Velocity (m/s), -A = Attenuation (-dB), -R = Root Means Square (volt), -Z = Impedance (10<sup>-3</sup> Gg/s-m<sup>2</sup>).

higher velocity than the NC method (Tables 1 and 2) for a given board type. This was probably because of impedance and frequency mismatch caused by pressurized gel-coupling process in the DC method. Such effects are absent in the NC method. The maximum amplitude of the transmitted wave occurs when the “acoustic impedances” of the media are matched. This kind of matching is required for a wave to be transmitted from one medium to another, for example, from liquid to solid (Benson 1991). This result is consistent with observations made by Bhardwaj (1997) and Bhardwaj et al. (2000) that DC ultrasonic velocities are always higher when working with viscoelastic, cellular, and powder-compact materials—particularly when liquids or gels are used as couplants. Under the current setup, the NC system produced a maximum velocity of 1270 m/s, compared with 1670 m/s from the

DC system for the same board type. The average impedance (a product of velocity and density) in the DC method had higher values than those from the NC method. For both methods, the impedance was significantly affected by the layering of boards.

Figure 3a shows a general nonlinear relationship between UT velocity and density. The regression curves between UT velocity and density (Fig. 3) showed the distinctive trends segregated by alignment levels for both methods. Particularly, the NC velocity models seemed effective in segregating the random, low, and high alignment levels in the high-density range. Meanwhile, the DC velocity models segregated the alignments well in the mid-density range. This observation suggested that both methods could produce a viable velocity-density model, if flake alignment parameter of the test material is known.

TABLE 2. Mechanical and ultrasonic properties for the three-layer boards at 4% RC level.

FWR <sup>a</sup>	Density (kg/m <sup>3</sup> )	Mechanical properties				Ultrasonic properties					
		MOR (MPa)	MOE (MPa)	RS (MPa·cm <sup>3</sup> )	EI (MPa·cm <sup>4</sup> )	DCV (m/s)	DCA (−dB)	DCR (v)	DCZ (Mg/s·m <sup>2</sup> )	NCV (m/s)	NCA (−dB)
High Alignment Level											
0.3	744 (48)	26.5 (3.0)	395 (23)	9.0 (1.3)	87 (2)	701 (90)	4.26 (4.3)	0.93 (0.19)	518 (41)	571 (27)	79.0 (4.9)
0.4	725 (18)	30.5 (3.1)	414 (19)	10.1 (1.1)	89 (4)	710 (35)	5.92 (4.2)	0.84 (0.21)	514 (24)	608 (48)	77.0 (2.8)
0.5	751 (43)	31.0 (2.5)	489 (48)	10.3 (0.8)	105 (10)	719 (24)	0.91 (0.7)	1.18 (0.10)	539 (21)	615 (22)	78.8 (3.8)
0.6	748 (31)	33.2 (3.1)	514 (49)	11.0 (0.7)	109 (7)	736 (65)	2.46 (3.0)	1.08 (0.24)	549 (46)	603 (32)	78.2 (1.3)
Low Alignment Level											
0.3	718 (46)	26.9 (3.3)	413 (56)	9.5 (1.3)	96 (14)	753 (60)	6.52 (8.7)	0.91 (0.37)	542 (75)	652 (38)	78.8 (2.9)
0.4	767 (49)	30.1 (3.2)	493 (73)	10.8 (1.8)	113 (8)	792 (46)	1.69 (2.6)	1.16 (0.26)	607 (49)	650 (19)	77.2 (6.5)
0.5	722 (82)	28.1 (6.7)	421 (117)	9.8 (2.2)	95 (25)	747 (53)	8.16 (11)	0.83 (0.30)	540 (78)	653 (77)	79.2 (2.6)
0.6	700 (23)	26.2 (3.3)	383 (33)	9.2 (1.2)	88 (8)	731 (46)	10.0 (14)	0.75 (0.35)	512 (42)	637 (61)	79.8 (5.3)

<sup>a</sup> Flake weight ratio between the face layers and the entire panel. Other notations are the same as shown in Table 1.

TABLE 3. Model parameters for ultrasonic DC and NC properties and panel density at the combined alignment level. Model  $Y = A + B \rho + C \rho^2 + D \rho^3$ , where  $Y$  = Velocity, Attenuation or RMS and density  $\rho$  in kg/m<sup>3</sup>. Significant parameters were evaluated by the backward elimination procedure at the 10% significant level.

UT <sup>a</sup> parameter	Panel type <sup>b</sup>	Regression coefficient <sup>c</sup> (combined value <sup>d</sup> )				R <sup>2</sup>
		A	B	C	D	
Velocity (m/s)						
DC – Vel	1L4%RC	3909.46	−13.03615	1.67E−02	−6.42E−06	0.70
	3L4%RC	736.04	/	/	/	0.00
NC – Vel	1L4%RC	511.55	/	3.30E−04	/	0.64
	3L4%RC	624.4	/	/	/	0.00
Attenuation (−dB)						
DC – A	1L4%RC	251.23	−0.6785	6.08E−04	−1.80E−07	0.86
	3L4%RC	594.85	−1.5416	1.00E−03	/	0.47
NC – A	1L4%RC	173.53	−0.23536	1.34E−04	/	0.61
	3L4%RC	146.57	/	−4.06E−04	3.80E−07	0.12
Root means square (volt)						
DC – RMS	1L4%RC	−2.46	0.006518	−2.93E−06	/	0.83
	3L4%RC	−4.41	/	2.57E−05	−2.00E−08	0.37

<sup>a</sup> NC and DC denote non-contact and direct-contact methods, respectively.  
<sup>b</sup> 1L and 3L denote one- and three-layer boards, and 4%RC denotes 4% resin content.  
<sup>c</sup> / denotes eliminated non-significant coefficients.  
<sup>d</sup> Combined alignment and flake weight ratio for the 1L and 3L, respectively.



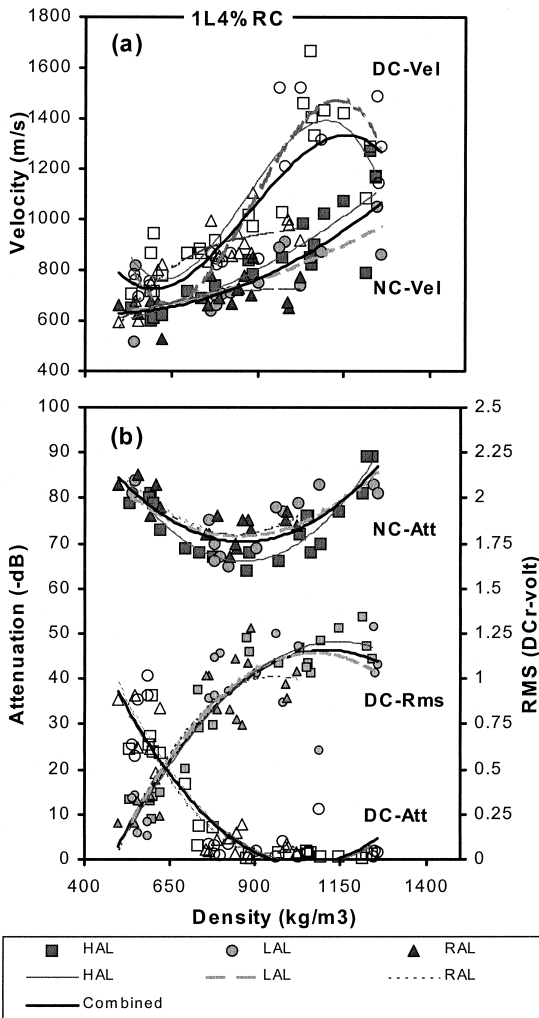


Fig. 3. Scatter plots of the velocity, attenuation, and RMS voltage (r) as a function of average panel density for 4% RC single-layer (1L) panels, segregated by DC and NC methods.

#### Attenuation/RMS-density correlation

Typical non-linear attenuation- and RMS-density relationships in the single-layer panels are shown in Fig. 3b for both methods. The NC attenuation decreased as the density increased, and reached a minimum at about 900 kg/m³. Above the density level, the NC attenuation increased as the density increased further. This indicates certain internal property changes as a result of densification under heat-

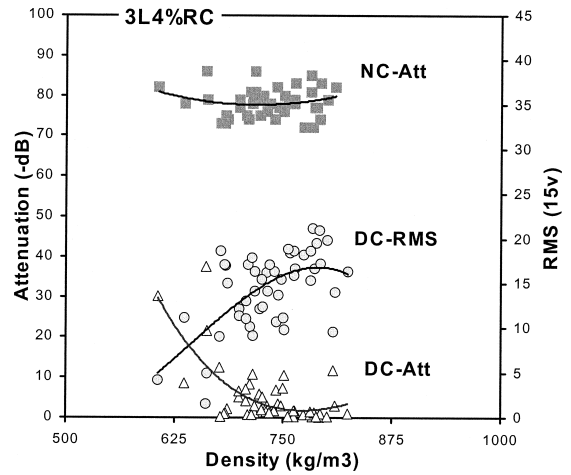


Fig. 4. Scatter plots of the DC and NC attenuation (Att) and DC RMS against density for the three-layer (3L) panels (combined shelling ratios) at the 4% RC level.

ing during hot pressing. The DC attenuation decreased and the DC RMS increased as the density increased. Above the 900 kg/m³ density point, both curves leveled off. This further indicates internal property changes above the density level. The density level showed the transition between the diminishing physical effects of the interspatial voids in the lower density half and the increasing plastic-strain hardening modifications in the higher density half. In contrast to the difference in UT velocity, the three-layer panels had similar patterns of attenuation and RMS responses (Fig. 4) as those of single-layer panels.

The DC attenuation-density models had consistently higher  $R^2$  values than the NC attenuation-density models (Table 3). The predicted DC attenuation and RMS were invariant to flake alignment changes. This indicated that the DC attenuation and DC RMS were effective in detecting internal properties beyond physical impediments of interfacial boundary of the material. The DC RMS models, approximately inverse to the DC attenuation, showed a better correlation ( $R^2 \geq 0.98$ ) with density for the 1L4%RC panels.

#### Strength-density correlation

IB strength, bending stiffness (E-I), and breaking resistance (R·S) were highly corre-

lated with average density for all panels (Table 4). Figure 5 shows that the strength-density models fitted well with the experimental data at various alignment levels. Rising IB-density curves (combined alignment level) are seen in the panels. This shows a potential for IB improvement in the 1L4%RC panels by increasing resin content and/or density of the panel. Furthermore, a significant improvement of the IB strength can be realized by increasing alignment level from random to high (Fig. 5 and Table 1) at a given density level.

Both E-I and R-S were highly correlated to the average sample density ( $R^2 > 0.79$ ). The E-I-density correlations improved from random to high alignment boards (Table 4). The increasing E-I slopes with alignments (Fig. 5) indicate that higher bending stiffness could be achieved with higher flake alignments regardless of density level. However, the R-S-density curves have similar slopes and different intercepts for the different alignment levels, indicating that the intrinsic material strength rather than the flake alignment influences the breaking ruptures for all panel types.

*Panel strength-UT property correlation*

A quadratic polynomial regression was done to establish correlation between panel strength properties (i.e., IB, EI, and RS) and UT parameters (i.e., velocity, attenuation, and RMS). The model parameters are summarized in Table 5. The models, plotted in Fig. 6 and 7, were well fitted with the experimental data. As shown in Table 5, all three strength properties correlated better to the DC parameters (velocity, attenuation, and RMS) as compared with the NC parameters. This indicates that strength prediction based on DC measurements would be more accurate than the NC methods.

It can be seen from the plots in Fig. 6 that the relationships between the IB strength, EI, or RS and the UT velocity formed a similar trend as the strength-density relationship. There was a general linear relationship for velocity up to about 1250 m/s for both methods.

TABLE 4. Parameters for the polynomial model between mechanical properties and density for the single-layer 4%RC panels.<sup>a</sup>

Panel alignment	Internal bond strength				Bending stiffness				Breaking resistance			
	A	B	C	R <sup>2</sup>	A	B	C	R <sup>2</sup>	A	B	C	R <sup>2</sup>
Random	-0.000002	0.0044	-1.4204	0.76	0.0005	-0.5673	174.2	0.89	8E-06	0.0125	-6.5543	0.97
Low	-3E-08	0.0013	-0.1555	0.85	0.00008	0.1654	.82889	0.82	-0.00001	0.0463	-14.601	0.87
High	-0.000003	0.0073	-2.4965	0.88	0.0003	-0.1057	14.682	0.96	-0.00001	0.0467	-13.486	0.96
Combined	-0.000001	0.0037	-1.1138	0.78	0.0003	-0.1681	34.335	0.87	-2E-06	0.0283	-9.1633	0.79

<sup>a</sup> Model  $Y = AX^2 + BX + C$ , where  $Y$  = internal bond (IB, MPa), bending stiffness (E-I, MPa-cm<sup>4</sup>), or breaking resistance (R-S, MPa-cm<sup>3</sup>), and  $X$  = average density (kg/m<sup>3</sup>).

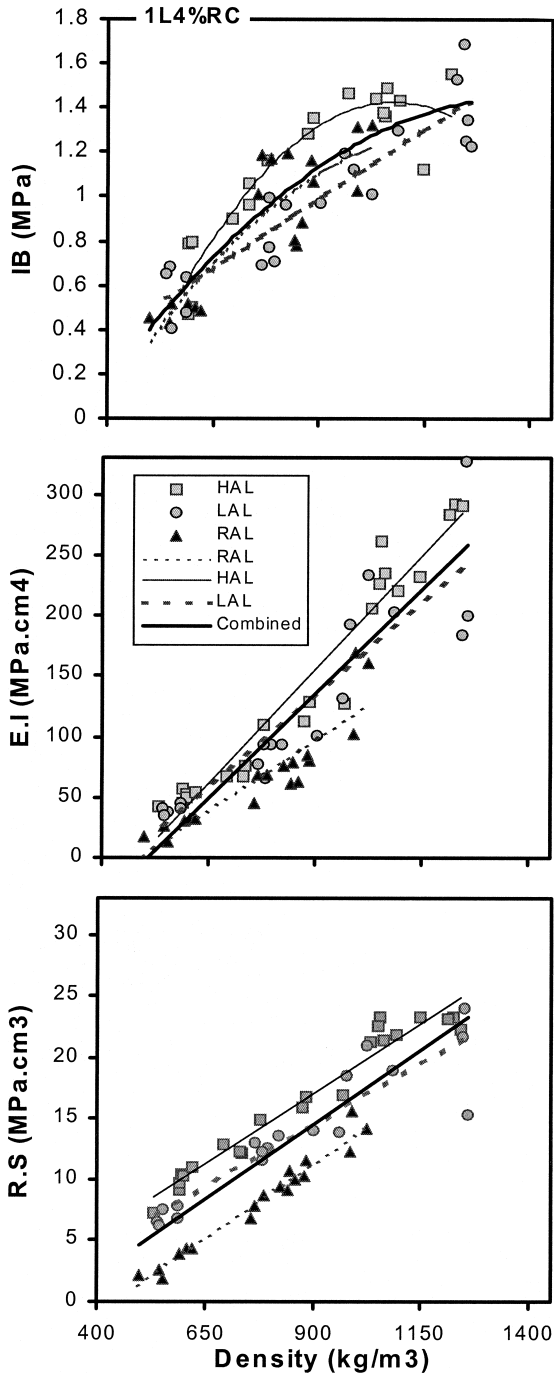


Fig. 5. Scatter plots of internal bond (IB), bending stiffness (E·I), and breaking resistance (R·S) versus density for single-layer boards, segregated by high (HAL), low (LAL), and random (RAL) alignment levels.

Beyond that velocity, the DC curves leveled off significantly indicating that all strength properties became independent of the UT velocity in the density range. The flake alignment levels showed little effects on the relationship. There was also a similar general trend for the NC data.

All three mechanical properties (i.e., IB, EI, and RS) showed an increased trend with DC RMS and a decreasing trend with DC attenuation (Fig. 7). The relationship is generally nonlinear (Table 5). The mechanical properties showed an inconsistent trend with NC attenuation for boards at all flake alignment levels. Flake alignment levels did not significantly influence the UT measurements from both DC and NC methods. Thus, under the current NC settings, strength prediction based on NC attenuation would be inaccurate for OSB products. In the three-layer boards, the NC attenuation showed invariant responses to the panel shelling ratio (i.e., FWR in Table 2). However, the DC attenuation had a minimum value at FWR = 0.5 for the high alignment boards; whereas, the DC RMS had a maximum value.

#### UT parameter-panel property interactions

Table 6 shows the results of the sensitivity analysis through the backward elimination procedure to show the interactions among the panel properties and UT parameters as influenced by high and low densities in the thickness and horizontal planes of each sample. The average density was strongly correlated to the low and high thickness densities. The low density in both planes significantly affected the bending stiffness of the high-alignment panels. As expected, the high stress concentration was formed in the low density ranges, leading to the bending fracture.

Velocity, in general, was significantly restrained by the low-density points in the thickness direction, especially for the high alignment panels. It was significantly dependent on the high-density area in the horizontal plane for propagation. Particularly, the low-vertical and high-horizontal densities restrained NC

TABLE 5. Parameters for panel strength and UT property models for the single-layer 4%RC boards.<sup>a</sup>

Y	Align level	DC – velocity (m/s)				NC – Velocity (m/s)			
		A	B	C	R <sup>2</sup>	A	B	C	R <sup>2</sup>
IB	Random	–2.E–06	0.0044	–1.6712	0.55	–6.E–06	0.0097	–3.1715	0.24
	Low	–3.E–06	0.0065	–2.8514	0.88	–6.E–07	0.0022	–0.3998	0.63
	High	–2.E–06	0.0054	–2.1862	0.61	–4.E–06	0.0083	–2.9333	0.78
	Combined	–2.E–06	0.0052	–2.1413	0.65	–2.E–06	0.0053	–1.6737	0.57
EI	Random	–2.E–04	0.5357	–246.76	0.46	–5.E–04	0.8508	–293.85	0.12
	Low	–7.E–04	1.7473	–886.85	0.79	–3.E–04	0.7144	–267.94	0.42
	High	–4.E–04	1.1565	–615.66	0.77	–5.E–04	1.3426	–579.53	0.74
	Combined	–3.E–04	0.831	–433.95	0.71	–1.E–04	0.6371	–287.61	0.61
RS	Random	–2.E–05	0.0581	–26.673	0.69	–2.E–05	0.0605	–21.69	0.23
	Low	–4.E–05	0.1064	–48.538	0.78	–1.E–06	0.0244	–3.752	0.42
	High	–2.E–05	0.0693	–30.055	0.87	–6.E–05	0.1256	–46.393	0.82
	Combined	–2.E–05	0.0687	–31.565	0.76	–3.E–05	0.0753	–28.095	0.58

<sup>a</sup> Model  $Y = AX^2 + BX + C$ , where  $Y$  = internal bond strength (IB, MPa), bending stiffness (E.I.,  $\text{MPa}\cdot\text{cm}^4$ ), or breaking resistance (R.S.,  $\text{MPa}\cdot\text{cm}^3$ );  $X$  = Velocity (m/s), Attenuation (–dB), or RMS (v).

velocity. This suggests that the high-horizontal density facilitated the tortuosity of velocity flux into the material, taking paths hindered by the bottleneck of the lowest thickness density portion. It appeared to present a “path of the least resistance” for the wave energy regardless of the original direction of the wave (also observed by Dickens et al. 1996). The DC attenuation and RMS behaved in a similar

manner. The energy loss in attenuation for both methods was caused by reflections along the high- and low-density boundaries in the thickness direction, and by lateral scattering along the horizontal density plane.

CONCLUSIONS

Through-thickness DC and NC ultrasonic transmission responses were used successfully

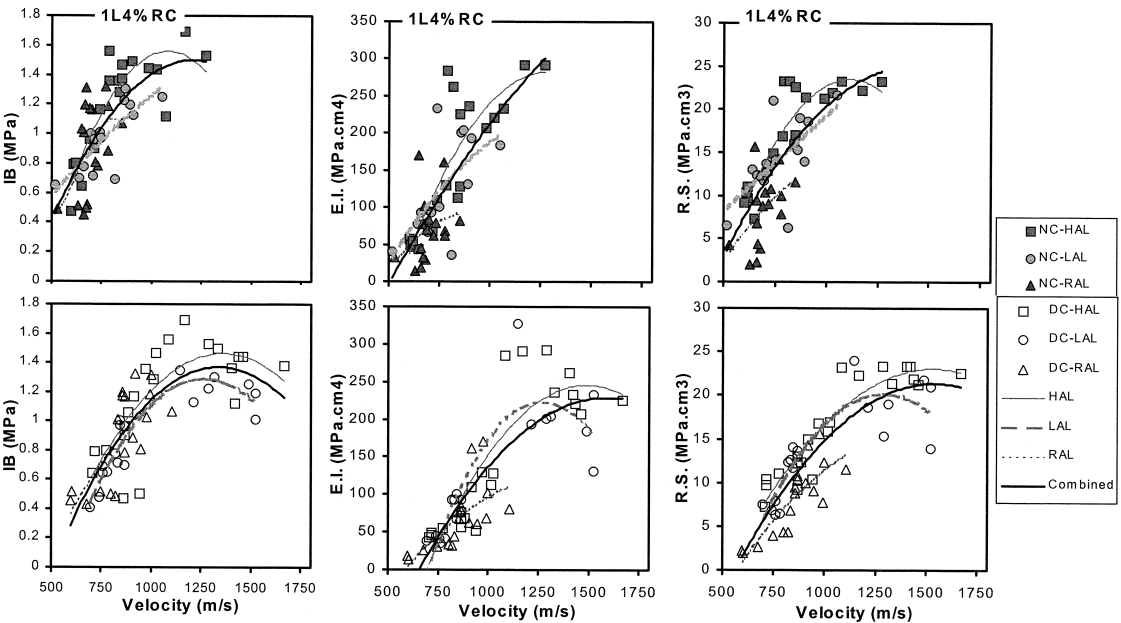


Fig. 6. Scatter plots of DC and NC velocities versus IB, E.I. and R.S. for single-layer, 4% RC boards, segregated by high (HAL), low (LAL), and random (RAL) alignment levels.

TABLE 5. *Extended.*

DC – Attenuation (dB)				NC – Attenuation (dB)				DC – RMS (v)			
A	B	C	R <sup>2</sup>	A	B	C	R <sup>2</sup>	A	B	C	R <sup>2</sup>
0.0006	–0.044	1.2006	0.81	–0.0033	0.4664	–15.394	0.45	–0.7664	1.8303	0.0329	0.79
–0.0002	–0.0077	1.0558	0.53	–0.0005	0.0888	–2.7437	0.12	–0.4449	1.1318	0.3565	0.53
0.0005	–0.0436	1.4392	0.84	0.0031	–0.4798	19.323	0.24	–0.6341	1.8352	0.1276	0.84
0.0004	–0.0342	1.2511	0.66	0.0017	–0.2628	11.105	0.06	–0.3256	1.218	0.2659	0.67
0.0712	–4.7309	101.12	0.49	–0.572	83.914	–2992.7	0.28	–105.22	223.64	–28.434	0.47
0.0417	–4.9312	162.35	0.34	–0.35	55.617	–2064.2	0.16	–92.287	245.65	–2.2581	0.34
0.2998	–14.82	220.79	0.64	0.4091	–58.047	2188.7	0.18	118.97	14.777	31.077	0.68
0.1659	–9.6383	171.02	0.42	0.3457	–49.991	1909.7	0.07	74.356	41.141	22.96	0.45
0.0054	–0.4483	11.726	0.71	–0.0532	7.6543	–265.28	0.46	–10.586	23.827	–2.5095	0.70
0.0048	–0.4519	17.052	0.52	–0.024	3.696	–126.74	0.05	–5.4168	17.237	4.0763	0.52
0.0181	–0.9359	21.279	0.77	0.0217	–3.206	134.26	0.06	3.6106	7.5363	6.8702	0.79
0.0103	–0.6775	17.336	0.49	0.024	–3.6606	151.87	0.03	3.408	7.0564	4.6268	0.53

to characterize OSB's basic properties as influenced by processing variables. All UT responses in relation to the sample density were distributed nonlinearly. DC velocity was higher than the NC velocity, presumably because of transducer or liquid couplant compression effects in the DC method and agglomeration of surfaces as affected by heat and pressure treatments. Generally good models in the single-layer boards were attributed to the nature of the internal structure defined by the uniform density profile and the mean larger density range. The ultrasonic properties were not affected by the panel shelling ratios for the three-layer boards.

The unique DC velocity and NC attenuation responses approaching the inflection density (900 kg/m<sup>3</sup>) indicated the diminishing effects of the physical voids in the low-density half and the strain hardening in the high-density half. The facts attested that the processing formulation in panel manufacturing, particularly high-density panels, could have definite effects on ultrasonic properties. The strength properties of the boards generally increased with density and flake alignment levels. Viable density models devised in either method were board-specific. Attenuation and RMS were an effective predictor of density if flake alignment level was not known; otherwise the UT velocity could be used.

High density–strength correlations were ob-

served for all board types. The bending stiffness correlated highly to low density points in both thickness and horizontal directions, whereas the breaking resistance correlated well to high sample density. Velocity from both methods depended significantly on the low thickness density, whereas the attenuation/RMS was significantly affected by high and low density boundaries in the thickness direction. The high correlations in both UT–strength and UT–density relationships signal that UT techniques can provide a quick effective assessment of OSB's internal characteristics.

Although the NC system does provide a suitably remote measurement convenience, we recommend that the instrumentation setup and calibration consideration need to match the natural frequency of the test material. With a proper calibration technique, the ultrasonic method is an effective tool for wood composite research and for on-line quality monitoring in fiber-based facilities.

#### ACKNOWLEDGMENTS

The financial support to this project by USDA NRI Competitive Grant Program (99-351103-8298) is gratefully acknowledged. The authors wish to thank the SecondWave System Corporation for providing the non-contact ultrasonic transmission measurements,

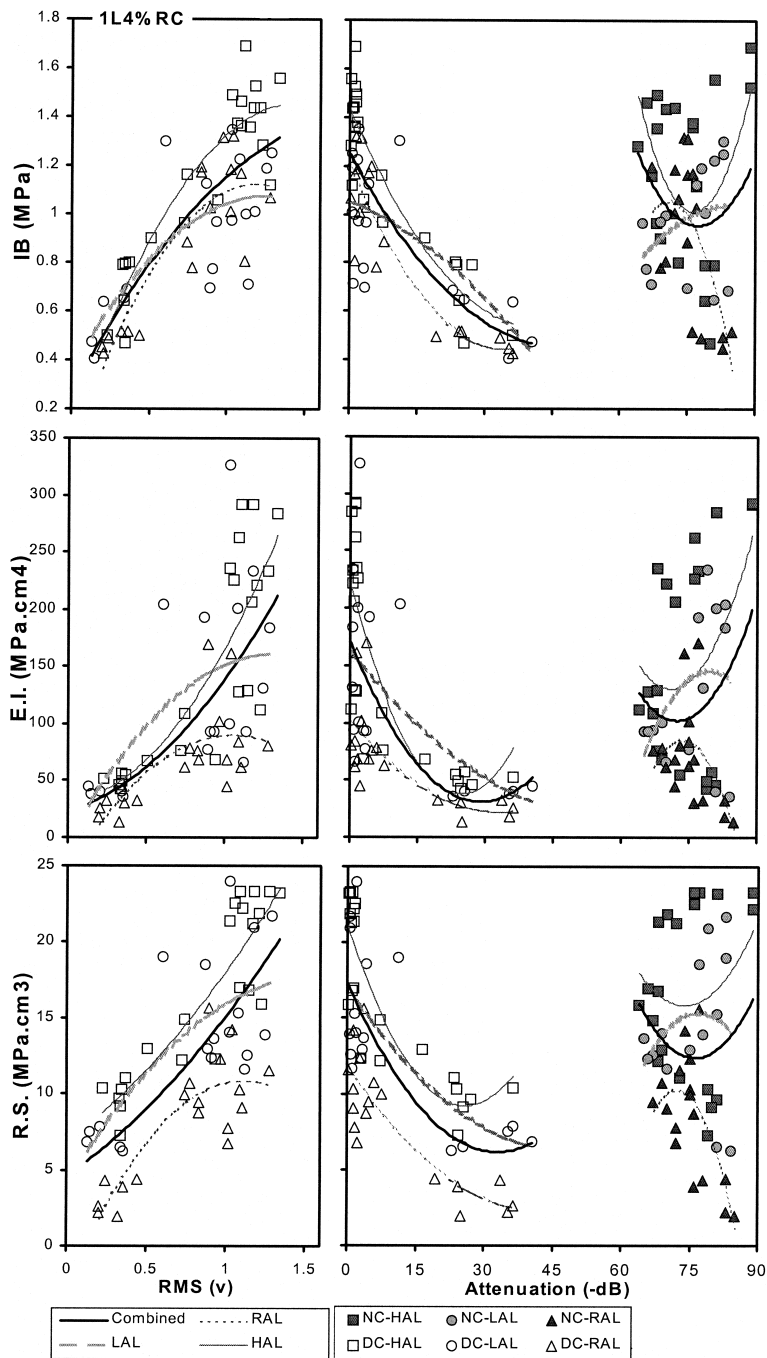


Fig. 7. Scatter plots of NC attenuation, DC RMS and DC attenuation versus IB, E.I. and R.S. for single-layer, 4% RC boards, segregated by high (HAL), low (LAL), and random (RAL) alignment levels.



TABLE 6. *Sensitivity test (in p-values) using backward elimination procedure to evaluate levels of interactions and influences among the structural properties and UT parameters in the high and low densities areas along the thickness and horizontal planes for 4% RC panels.*

Variables	Alignment level	Vertical-Thickness		Horizontal-Plane	
		Density High	Density Low	Density High	Density Low
Stiffness (E.I.)	Combined	0.0929	NS	NS	0.0001
	Random	NS	NS	NS	0.0001
	Low	NS	NS	NS	0.0001
	High	NS	0.0001	NS	NS
Breaking (R.S.)	Combined	NS	NS	NS	0.0001
	Random	0.0001	NS	NS	NS
	Low	NS	NS	NS	0.0001
	High	NS	NS	0.0001	NS
Ave_Density	Combined	0.0001	0.0001	NS	0.0018
	Random	0.0001	0.002	NS	NS
	Low	0.0036	0.0001	NS	0.0401
	High	0.017	0.0413	0.0012	0.0099
DC_Velocity	Combined	NS	0.0001	NS	NS
	Random	0.0001	NS	NS	NS
	Low	0.018	NS	0.001	NS
	High	NS	0.0001	NS	NS
DC_Attenuation	Combined	0.0022	0.0005	0.01	NS
	Random	NS	0.0001	NS	0.0156
	Low	0.0003	0.0038	NS	NS
	High	NS	NS	0.0001	NS
DC_RMS	Combined	0.0058	0.0161	0.0722	NS
	Random	NS	0.0001	NS	NS
	Low	0.0036	0.038	NS	NS
	High	NS	NS	0.0001	NS
NC_Velocity	Combined	NS	0.0001	0.0132	NS
	Random	NS	0.0397	NS	NS
	Low	NS	NS	0.0016	NS
	High	NS	0.0001	NS	NS
NC_Attenuation	Combined	0.0012	0.0001	0.0958	NS
	Random	0.0006	NS	NS	0.0098
	Low	0.0001	0.0001	NS	NS
	High	NS	0.0088	0.0105	NS

and Dr. Aravamudhan Raman, Department of Mechanical Engineering, Louisiana State University, for his helpful suggestions.

#### REFERENCES

- AMERICAN SOCIETY FOR TESTING AND MATERIALS (ASTM). 1996. Annual Book of ASTM Standard D1037-96, American Society for Testing and Materials, Philadelphia, PA.
- BEALL, C. F. 1996a. Application of ultrasonic technology to wood and wood-based materials. *In* Ferenc Divos, ed. Proc. 2nd University of Western Hungary International Conference on the Wood Science/Technology and Forestry. Sopron, Hungary.
- . 1996b. Future of nondestructive evaluation of wood and wood-based materials. Keynote pages 409–413 *in* Proc. 10th International Conference on NDE of Civil Structures & Materials, Boulder, CO.
- BEAUCHAMP, K. G., AND C. K. YUEN. 1979. Digital methods for signal analysis. George Allen & Unwin Ltd., Boston, MA.
- BENSON, H. 1991. University physics. John Wiley & Sons, New York, NY. pp. 663–672; 962 pp.
- BHARDWAJ, M. C. 1997. Innovation in non-contact ultrasonic analysis: Applications for hidden objects detection. *Mat. Res. Innovation* 1:188–196.
- , I. NEESON, AND G. STEAD. 2000. Introduction to contact-free ultrasonic characterization and analysis of consolidated materials. Technical report at the Application of Nondestructive Evaluation in Powder Metals Seminar. Iowa State Univ., Ames, IA. 13 pp.

- CHEN, L.-H., AND F. C. BEALL. 2000. Monitoring bond strength development in particleboard during pressing, using acousto-ultrasonics. *Wood Fiber Sci.* 32(4):466–477.
- DICKENS, J. R., D. A. BENDER, AND D. E. BRAY. 1996. A critical-angle ultrasonic technique for inspection of wood parallel-to-grain. *Wood Fiber Sci.* 28(3):380–388.
- ERMOLOV, I. N. 1998. Major ultrasonic inspection problem. *Russian J. Nondestructive Testing* 34(1):35–37. Plenum Publishing, New York, NY.
- FURUNO, T., C.-Y. HSE, AND W. A. COTE. 1983. Observation of microscopic factors affecting strength and dimensional properties of hardwood flakeboard. Pages 297–312 in T. M. Maloney, ed. *Proc. 17th Washington State University International Symposium on Particleboard-Composite Materials*. Pullman, WA.
- GEIMER, R. L. 1979. Data basic to engineering design of reconstituted flakeboard. Pages 105–125 in T. M. Maloney, ed. *Proc. 13th Washington State University International Symposium on Particleboard/Composite Materials*. Pullman, WA.
- JEONG, H. 1997. Effects of voids on the mechanical strength and ultrasonics attenuation of laminated composites. *J Composite Mater.* 31(3):276–292.
- , AND D. K. HSU. 1995. Experimental analysis of porosity-induced ultrasonic attenuation and velocity change in carbon composites. *Ultrasonics* 33(3):195–203.
- JUDD, N. C. W., AND W. W. WRIGHT. 1978. Voids and their effects on the mechanical properties of composites—An appraisal. *SAMPE Journal*, January/February: 10–14.
- LEE, N. J., AND Q. WU. 2002. In-plane dimensional stability of three-layer oriented strandboard. *Wood Fiber Sci.* 34(1):77–95.
- LENTH, C. A., AND F. A. KAMKE. 1996. Investigations of flakeboard mat consolidation. Part I. Characterization the cellular structure. *Wood Fiber Sci.* 28(2):153–167.
- SAS INSTITUTE INC. 2000. SAS User's Guide version 8.0. SAS Institute Inc., Cary, NC.
- VUN, R. Y.-H. 1998. Monitoring creep rupture in oriented strandboard using acoustic emission FPL rep. 36-01-138, University of California Forest Product Laboratory, Richmond, CA. 87 pp.
- , Q. WU, M. C. BHARDWAJ, AND G. STEAD. 2000. Through-thickness ultrasonic transmission properties of oriented strandboard. Pages 77–86 in Ferenc Divos, ed. *Proc. 12th University of Western Hungary International Symposium on Nondestructive Testing of Wood*. Sopron, Hungary.
- WU, Q. 1999. In-plane dimensional stability of oriented strand panel: Effect of processing variables. *Wood Fiber Sci.* 31(1):28–40.